BIFURCATION CHARACTERISTICS AND BURSTING OSCILLATION OF DUFFING-VAN DER POL OSCILLATOR

by

FengXia WU[a,b*] and ZiTian LI[b*]

[a]Faculty of Civil Engineering and Mechanics, Kunming University of Science and Technology, Kunming, China
[b]School of Mathematics and Economics, Qujing Normal University, Qujing, China

Original scientific paper
https://doi.org/10.2298/TSCI2503849W

In this paper, we study the bifurcation characteristics and bursting oscillation of the Duffing-Van der Pol system with periodic excitation. Due to the different frequency scales between the excitation frequency and the natural frequency in the oscillator, when the periodic excitation changes slowly with time, the system is considered as a slow subsystem, and when it is fixed, the system is considered as a fast subsystem. We analyze the bifurcation characteristics of the fast subsystem and use the slowly varying parameter as the bifurcation parameter to show how the bursting oscillations are generated. Furthermore, the phase diagram and time-history diagram of fold-fold bursting oscillation, fold-subHopf bursting oscillation, supHopf-supHopf bursting oscillation, and homoclinic-homoclinic bursting oscillation are given by numerical simulation. Combined with the figures, it is found that these four kinds of bursting oscillations with bifurcation delay phenomenon are symmetrical and further reveal the bifurcation mechanisms of these four kinds of bursting oscillations.

Key words: *fast-slow dynamics, fold bifurcation, homoclinic bifurcation, Hopf bifurcation*

Introduction

Multi-time-scale non-linear dynamical problems are an important component of non-linear scientific research, which is very different from the dynamic behavior of systems on a single time scale. The study of multi-time scale problems can be traced back to the analysis of boundary layer fluid characteristics [1]. With the rapid development of modern science and engineering technology, more and more multi-time-scale non-linear dynamic problems have emerged. For example, vibration energy harvesters [2], chemical systems [3], aircraft systems [4], electromechanical systems [5], and so on.

Van der Pol oscillator [6, 7] and Duffing oscillator [8, 9] are both non-linear systems with important application background and are well-known models in mechanics and physics. The Duffing-Van der Pol equation combines the features of the Duffing oscillator (non-linear spring force) and the van der Pol oscillator (non-linear damping force) [10, 11]. Analytical solutions of such equation are difficult to obtain though we have some famous analytical methods for simple non-linear oscillators, for examples, the homotopy perturbation method [12-14], the variational iteration method [15, 16], He’s frequency formulation [17, 18], so various numerical

* Corresponding authors, e-mail: 252925990@qq.com; 1753150687@qq.com

methods were appeared to study such complex problems, however, all numerical approaches requires given parameters and given initial conditions [19], this requirement makes dynamical analysis difficult, it can not figure out some important criteria for periodic motion [8, 9], chaotic motion [20-22], pull-in motion [23-25], and bifurcation [7]. The pull-in instability is extremely studied in micro-electromechanical systems for safe and reliable operation [26-28]. The study of the Duffing-Van der Pol equation is often associated with non-linear dynamics and chaos theory. The equation exhibits a rich variety of dynamical behaviors, including periodic motion, bifurcations, chaos, and strange attractors. The system has both fast and slow time scales. The fast oscillations are associated with the natural frequencies of the system, while the slow variations occur due to parameter changes or external forcing. In summary, the slow-fast dynamics of the Duffing-Van der Pol equation involves the coexistence of fast oscillations and slow variations, and the analysis of these dynamics is essential for understanding the behavior of the system, especially in the presence of bifurcations and complex non-linear phenomena.

Description of the equation and bifurcation characteristics

The description of the equation

In this paper, we consider the non-autonomous Duffing-Van der Pol oscillator described [11]:

$$\begin{aligned}\dot{x} &= y \\ \dot{y} &= -\alpha x - \beta x^3 - \mu(1-x^2)y + \gamma\cos(\omega t)\end{aligned} \tag{1}$$

where x, y denote the state variables, the dot means the differentiation of the time t, α, β, $\mu = O(1)$ are real parameters, and γ and ω $(0 < \omega << 1)$ are the amplitude and frequency of the external excitation, respectively.

In order to reveal the fast-slow bursting behaviors of the system (1), defining the new parameter $F = \gamma\cos(\omega t)$, system (1) becomes:

$$\begin{aligned}\dot{x} &= y \\ \dot{y} &= -\alpha x - \beta x^3 - \mu(1-x^2)y + F\end{aligned} \tag{2}$$

From the perspective of the slow-fast analysis, there is an order magnitude gap between excitation frequency ω and natural frequency Ω. The system (2) is regarded as the fast subsystem and system (1) is the slow subsystem.

The equilibrium point and its stabilities

From system (2), we can acquire the equilibrium point $E(x_0, 0)$ satisfies the following cubic equation of one variable:

$$\beta {x_0}^3 + \alpha x_0 - F = 0 \tag{3}$$

The Cardan formula [29] is used to find the roots of the eq. (3). When $\Delta > 0$, eq. (3) has one real root $x_0 = A^{1/3} + B^{1/3}$; when $\Delta = 0$, eq. (3) has two real roots $x_0 = 2A^{1/3}$ or $x_0 = -A^{1/3}$; when $\Delta < 0$, eq. (3) has three real roots $x_0 = A^{1/3} + B^{1/3}$ and:

$$x_0 = \left(-\frac{1}{2} \pm \frac{\sqrt{3}i}{2}\right)A^{\frac{1}{3}} + \left(-\frac{1}{2} \mp \frac{\sqrt{3}i}{2}\right)B^{\frac{1}{3}}$$

in which:

$$\Delta=\frac{F^2}{4\beta^2}+\frac{\alpha^3}{27\beta^3},\quad A=\frac{F}{2\beta}-\Delta^{\frac{1}{2}},\quad B=\frac{F}{2\beta}+\Delta^{\frac{1}{2}}$$

The stabilities of equilibrium points can be decided by the linearization theory. Linearizing system (2) at $E(x_0,0)$, we can gain the following Jacobian matrix:

$$J=\begin{bmatrix}0 & 1\\ -\alpha-3\beta x_0^2 & -\mu(1-{x_0}^2)\end{bmatrix}\tag{4}$$

and its characteristic equation can be expressed:

$$\det\begin{bmatrix}\lambda & -1\\ \alpha+3\beta x_0^2 & \lambda+\mu(1-{x_0}^2)\end{bmatrix}=\lambda^2+\mu(1-{x_0}^2)\lambda+\alpha+3\beta x_0^2=0\tag{5}$$

According to the Routh-Hurwitz criterion [30], we can gain the following stability conditions:

$$\mu(1-{x_0}^2)>0,\quad \alpha+3\beta x_0^2>0,\quad \beta {x_0}^3+\alpha x_0-F=0\tag{6}$$

By adjusting the value of parameters, the stability condition is not satisfied, different types of bifurcation may appear which will result in different patterns of bursting oscillations.

Fold bifurcation

Fold bifurcation [31] can cause the jumping phenomenon between different equilibrium points. According to eq. (5), the conditions of fold bifurcation is obtained:

$$\alpha+3\beta x_0^2=0,\quad \beta {x_0}^3+\alpha x_0-F=0\tag{7}$$

Eliminating x_0, we have:

$$4\alpha^3+27\beta F^2=0\tag{8}$$

In this case, eq. (5) has two roots written as $\lambda_1=0$ and $\lambda_2=-\mu(1-{x_0}^2)$, which means the occurrence of fold bifurcation.

Hopf bifurcation

Hopf bifurcation [32] can cause the occurrence of a limit cycle which leads to the periodic bursting oscillation. Substituting $\lambda=\pm i\omega$ into eq. (5) and eliminating ω, then the first condition of Hopf bifurcation generated by $E(x_0, 0)$:

$$x_0^2=1,\quad \omega^2=\alpha+3\beta>0,\quad F=(\alpha+\beta)x_0\tag{9}$$

Taking the partial derivatives in both sides of eqs. (5) and (3) with respect to F, letting $\lambda=i\omega$ and separating the real part of ($\mathrm{d}\lambda/\mathrm{d}F$), we have the following second condition of Hopf bifurcation:

$$\mathrm{Re}\left(\frac{\mathrm{d}\lambda}{\mathrm{d}F}\right)=\frac{4\mu x_0\omega^2-6\mu\beta x_0(1-x_0^2)}{(3\beta x_0^2+\alpha)[4\omega^2+\mu^2(1-x_0^2)^2]}=\frac{\mu F}{(\alpha+\beta)(3\beta+\alpha)}\neq 0\tag{10}$$

The second condition of Hopf bifurcation is also satisfied. So, it is proved that Hopf bifurcation will occur in the system (2). In order to judge the types of Hopf bifurcations, we need to calculate the first Lyapunov coefficient $l_1(0)$. By linear transformation, the equilibrium point $E(x_0, 0)$ is shifted to the origin point (0, 0), system (2) can be rewritten:

$$\begin{pmatrix} \dot{x} \\ \dot{y} \end{pmatrix} = J \begin{pmatrix} x \\ y \end{pmatrix} + \begin{pmatrix} 0 \\ -3\beta x_0 x^2 + 2\mu x_0 xy + \mu x^2 y - \beta x^3 \end{pmatrix} \tag{11}$$

Then we compute the eigenvectors q and p of Matrix J and J^T, which satisfy $Jq = i\omega q,\ J^T p = -i\omega p$ and $< p, q >= 1$, where J^T is the transposed matrix of J and $<\cdot,\cdot>$ is the standard scalar product in R^2. By computation, we have:

$$p = \left(\frac{1}{2}, \frac{i}{2\omega}\right)^T, \quad q = (1, i\omega)^T \tag{12}$$

The bilinear and trilinear functions are:

$$\begin{aligned} B(x,y) &= \begin{bmatrix} 0 \\ -6\beta x_0 x_1 y_1 + 2\mu x_0 (x_1 y_2 + x_2 y_1) \end{bmatrix} \\ C(x,y,z) &= \begin{bmatrix} 0 \\ 2\mu(x_1 y_1 z_2 + x_1 y_2 z_1 + x_2 y_1 z_1) - 6\beta x_1 y_1 z_1 \end{bmatrix} \end{aligned} \tag{13}$$

So, the first Lyapunov coefficient is:

$$l_1(0) = \frac{1}{2\omega} \left\{ \begin{aligned} &< p, C(q,q,\bar{q}) > -2 < p, B[q, A^{-1}B(q,\bar{q})] > \\ &+ < p, B[\bar{q}, (2i\omega E - A)^{-1} B(q,q)] > \end{aligned} \right\} = \frac{\mu}{2\omega} \frac{\alpha - 3\beta}{\alpha + 3\beta} \tag{14}$$

When $\mu(\alpha - 3\beta) < 0,$ a stable supercritical Hopf bifurcation occurs. When $\alpha = 3\beta,$ co-dimension-2 degenerate Hopf bifurcation occurs. When $\mu(\alpha - 3\beta) > 0,$ an unstable subcritical Hopf bifurcation occurs.

Melnikov analysis for heteroclinic and homoclinic bifurcations

As known to all, Melnikov method presents a procedure to calculate the parameter conditions of the homoclinic and heteroclinic bifurcations to chaos [33].

The perturbed system (1) is written:

$$\begin{aligned} \dot{x} &= y \\ \dot{y} &= -\alpha x - \beta x^3 - \varepsilon[\mu(1 - x^2) y - \gamma \cos(\omega t)] \end{aligned} \tag{15}$$

which corresponds to an integrable Hamiltonian system given by:

$$\begin{aligned} \dot{x} &= y \\ \dot{y} &= -\alpha x - \beta x^3 \end{aligned} \tag{16}$$

whose associated the potential function is:

$$\delta(x) = \frac{\alpha x^2}{2} + \frac{\beta x^4}{4} \tag{17}$$

and Hamiltonian function is:

$$H(x,y)=\frac{y^2}{2}+\frac{\alpha x^2}{2}+\frac{\beta x^4}{4} \tag{18}$$

When $\alpha\beta<0,$, the system (16) has three fixed points (0, 0), $[\pm(-\alpha/\beta)^{1/2}$, 0]. Suppose $\alpha>0, \beta<0,$ because:

$$\delta''(0)=\alpha>0, \qquad \delta''\left[\pm\left(-\frac{\alpha}{\beta}\right)^{\frac{1}{2}}\right]=-2\alpha<0$$

so point (0, 0) is a center:

$$\left[\pm\left(-\frac{\alpha}{\beta}\right)^{\frac{1}{2}},0\right]$$

are saddles. The heteroclinic orbits connecting saddle points can be solved by:

$$\frac{\dot{x}^2}{2}+\frac{\alpha x^2}{2}+\frac{\beta x^4}{4}=0 \tag{19}$$

Set $t=0,\ \dot{x}(0)=0,$ we have:

$$x(0)=\pm\left(-\frac{2\alpha}{\beta}\right)^{\frac{1}{2}}$$

For a closed nodal energy (H = 0), performing the integration over eq. (19), we have:

$$\int_{x_0}^{x}\pm\frac{\mathrm{d}x}{\left(-\alpha x^2-\dfrac{\beta x^4}{2}\right)^{1/2}}=t \tag{20}$$

Then the heteroclinic orbits can be given by:

$$\begin{aligned}x_{\pm}^{0}(t)&=\pm\left(\frac{-\alpha}{\beta}\right)^{1/2}\tanh\left[\left(\frac{\alpha}{2}\right)^{1/2}t\right]\\ y_{\pm}^{0}(t)&=\pm\frac{\alpha}{(-2\beta)^{1/2}}\operatorname{sech}^2\left[\left(\frac{\alpha}{2}\right)^{1/2}t\right]\end{aligned} \tag{21}$$

According to the definition of Melnikov function, using eq. (21), the Melnikov integral of heteroclinic orbit is obtained:

$$M_{\mathrm{Hete}}(t_0)=\int_{-\infty}^{+\infty}\{-\mu[1-x_{\pm}^0(t)^2]y_{\pm}^0(t)+\gamma\cos[\omega(t+t_0)]\}y_{\pm}^0(t)\mathrm{d}t=$$

$$=-\mu\int_{-\infty}^{+\infty}y_{\pm}^0(t)^2\mathrm{d}t+\mu\int_{-\infty}^{+\infty}x_{\pm}^0(t)^2y_{\pm}^0(t)^2\mathrm{d}t+\gamma\cos(\omega t_0)\int_{-\infty}^{+\infty}\cos(\omega t)y_{\pm}^0(t)\mathrm{d}t= \tag{22}$$

$$=2\frac{\mu\alpha(5\beta+\alpha)(2\alpha)^{1/2}}{15\beta^2}\pm\pi\omega\gamma\cos(\omega t_0)\left(-\frac{2}{\beta}\right)^{1/2}\operatorname{csch}\left[\frac{\pi\omega}{(2\alpha)^{1/2}}\right]$$

where t_0 means the cross-section time of the Poincare map. Therefore, the necessary conditions for the occurrence of heteroclinic orbits in system (1) are:

$$|\gamma|>\left|2\mu\alpha(5\beta+\alpha)(-\alpha\beta)^{1/2}\frac{\sinh\left[\dfrac{\pi\omega}{(2\alpha)^{1/2}}\right]}{15\pi\omega\beta^2}\right|,\quad \left.\frac{\mathrm{d}M_{\mathrm{Hete}}}{\mathrm{d}t}\right|_{t=t_0}\neq 0 \tag{23}$$

When $\alpha<0, \beta>0$, because $\delta''(0)=\alpha<0$, $\delta''[\pm(-\alpha/\beta)^{1/2}]=-2\alpha>0$, so point (0, 0) is saddle, $[\pm(-\alpha/\beta)^{1/2}, 0]$, are centers. The homoclinic orbits connecting saddle points can be written as:

$$\begin{aligned}x_{\pm}^0(t)&=\pm\left(\frac{-2\alpha}{\beta}\right)^{1/2}\operatorname{sech}\left[(-\alpha)^{1/2}t\right]\\ y_{\pm}^0(t)&=\pm\alpha\left(\frac{2}{\beta}\right)^{1/2}\operatorname{sech}\left[(-\alpha)^{1/2}t\right]\tanh\left[(-\alpha)^{1/2}t\right]\end{aligned} \tag{24}$$

According to eq. (24), the Melnikov function of homoclinic orbit is given:

$$M_{\mathrm{Homo}}(t_0)=\int_{-\infty}^{+\infty}\left\{-\mu\left[1-x_{\pm}^0(t)^2\right]y_{\pm}^0(t)+\gamma\cos\left[\omega(t+t_0)\right]\right\}y_{\pm}^0(t)\mathrm{d}t$$

$$=-\mu\int_{-\infty}^{+\infty}y_{\pm}^0(t)^2\mathrm{d}t+\mu\int_{-\infty}^{+\infty}x_{\pm}^0(t)^2y_{\pm}^0(t)^2\mathrm{d}t+\gamma\sin(\omega t_0)\int_{-\infty}^{+\infty}\sin(\omega t)y_{\pm}^0(t)\mathrm{d}t=$$

$$=4\mu\alpha(-\alpha)^{1/2}\frac{(5\beta+4\alpha)}{15\beta^2}\mp\pi\omega\gamma\sin(\omega t_0)\left(\frac{2}{\beta}\right)^{1/2}\operatorname{sech}\left[\frac{\pi\omega}{2(-\alpha)^{1/2}}\right] \tag{25}$$

Therefore, the necessary conditions for the occurrence of cross-section of homoclinic orbits in system (1) are:

$$|\gamma|>\left|2\mu\alpha(5\beta+4\alpha)(-2\alpha)^{1/2}\frac{\cosh\left(\dfrac{\pi\omega}{2(-\alpha)^{1/2}}\right)}{15\pi\omega\beta^{3/2}}\right|,\quad \left.\frac{\mathrm{d}M_{\mathrm{Homo}}}{\mathrm{d}t}\right|_{t=t_0}\neq 0 \tag{26}$$

By calculating eqs. (23) and (26), system (1) will progress to chaotic motion *via* heteroclinic or homoclinic bifurcation which means the system (1) appears chaotic behaviors in the sense of smale's horseshoe [34].

Numerical simulations of bursting oscillations

System (1) is a multi-parameter dynamic system. In this part, the dynamical behavior of slow subsystem is numerically simulated by the stability and bifurcation of the fast subsystem.

Figures 1 and 2 show the phase diagram and time history diagram of system (1) at different excitation frequencies scales, respectively. It can be seen from fig. 1 that the system is chaotic motion and the system in fig. 2 is bursting oscillators. When the frequency is small, the chaotic motion of the system has hysteresis, which is a common phenomenon of bursting oscillators.

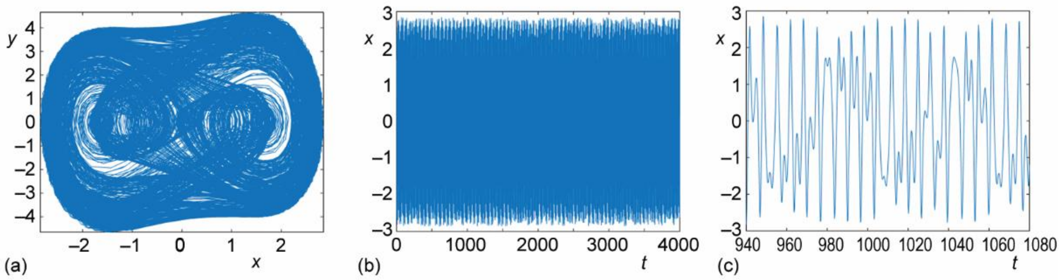

Figure 1. Chaotic motion of fast subsystem for β = 1, μ = –0.1, α = –1, γ = 3, and ω = 1; (a) phase portrait, (b) time history of x, and (c) locally enlarged image of the (b)

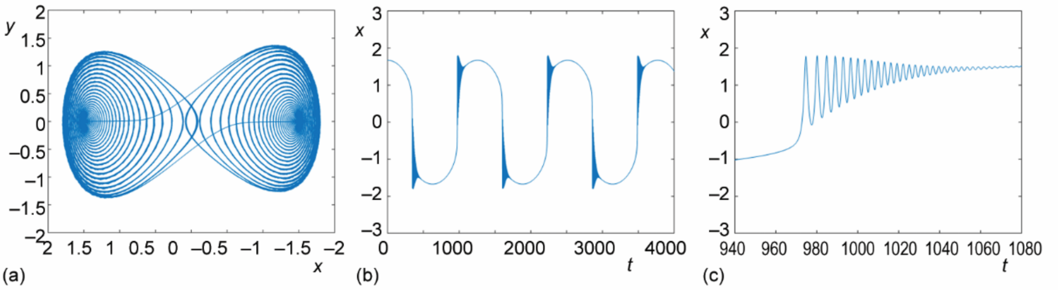

Figure 2. Bursting oscillators of slow subsystem for β = 1, μ = –0.1, α = –1, γ = 3, and ω = 0.005; (a) phase portrait, (b) time history of x, and (c) locally enlarged image of the (b)

In order to illustrate the bursting oscillators of system (1), so we take the parameters at $\beta = 1$, $\mu = -1$, $\omega = 0.005$ in the following. From the previous analysis, we know that the system (1) has four kinds of bifurcations: folding bifurcation, Hopf bifurcation, heteroclinic bifurcation, and homoclinic bifurcation. In addition, the number of equilibrium points changes correspondingly with the change of F.

The phase portrait, the corresponding time history and locally enlarged image of time history of fold-fold bursting oscillators are demonstrated in figs. 3(a)-3(d). Because of the fold bifurcation of the fast subsystem, the jumping phenomenon occurs, which causes the trajectory of the slow subsystem to jump back and forth between the upper and lower stable branches. During the whole period of bursting oscillation, adjusted by folding bifurcation, the trajectory undergoes the transition between two quiescent states and two spiking states.

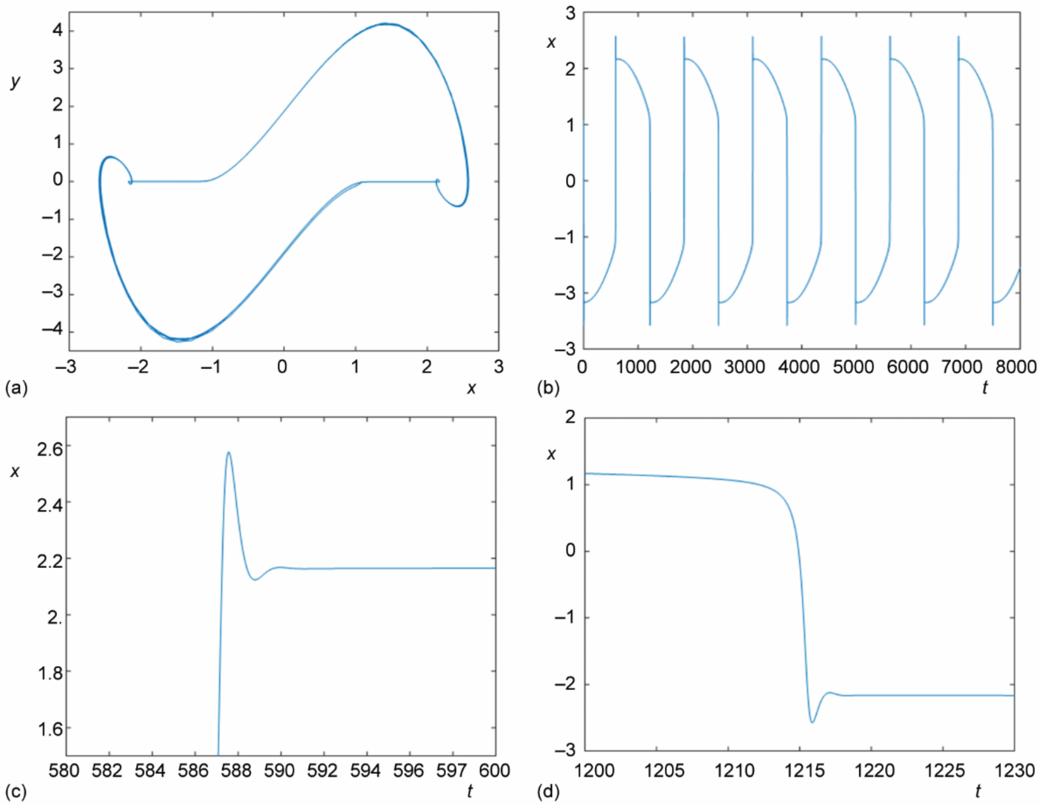

Figure 3. Fold-fold bursting oscillators for $\alpha = -3.5$, $\gamma = -2.6$; (a) phase portrait, (b) time history of x, (c) locally enlarged image of the (b), and (d) locally enlarged image of the (b)

Similarly, figs. 4(a)-4(c) show the phase portrait, the corresponding time history and locally enlarged image of time history of fold-subHopf bursting oscillators. It is found that the trajectory firstly moves to the point of subcritical Hopf bifurcation, then subcritical Hopf bifurcation occurs and the equilibrium point is unstable. However, because of the bifurcation delay, the trajectory of the system will continue to move around the equilibrium point, and after some distance, it will jump to another subcritical Hopf bifurcation point. At this point, the trajectory is half complete.

Figure 5 depicts the supHopf -supHopf bursting oscillators. From the figure, we can see two stable limit cycles generated by the supercritical Hopf bifurcation and the jump of the orbit at the two bifurcation points.

Figure 6 is the corresponding graph of homoclinic-homoclinic bursting oscillators. As we can see, when the orbit moves to the homoclinic bifurcation point, the delayed limit cycle is generated and gradually increased, and then absorbed by another homoclinic bifurcation point. The entire orbit is generated by two homoclinic bifurcation points and two hysteresis loops.

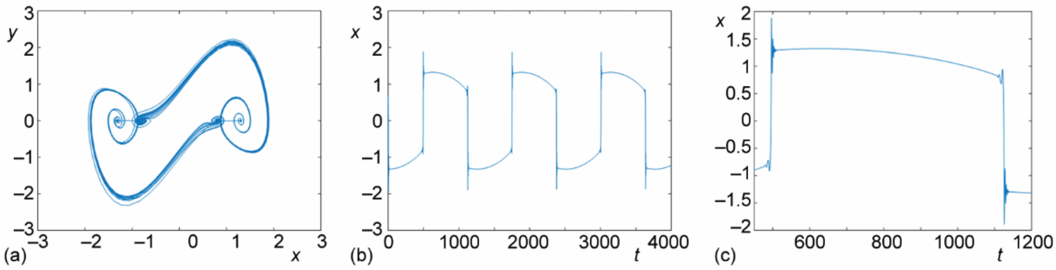

Figure 4. Fold-subHopf bursting oscillators for α = –1.4, γ = –0.65; (a) phase portrait, (b) time history of *x*, and (c) locally enlarged image of the (b)

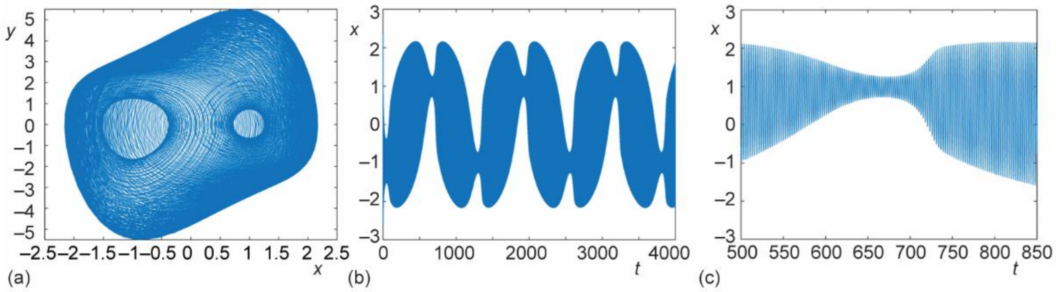

Figure 5. SupHopf -supHopf bursting oscillators for α = –3.5, γ = –4.6; (a) phase portrait, (b) time history of *x*, and (c) locally enlarged image of the (b)

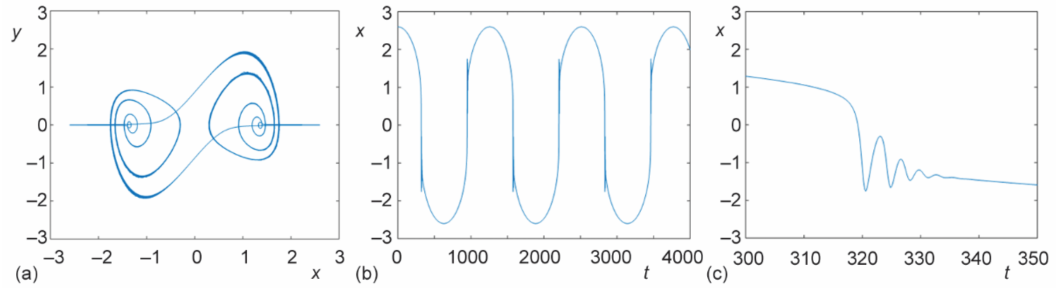

Figure 6. Homoclinic-homoclinic bursting oscillators for α = –0.8, γ = 15.5; (a) phase portrait, (b) time history of *x*, and (c) locally enlarged image of the (b)

Conclusion

This paper studies the fast-slow dynamics of the Duffing-Van der Pol system with slow varying periodic excitation. The theoretical analysis reveals the conditions for fold bifurcation, Hopf bifurcation, heteroclinic bifurcation, and homoclinic bifurcation, as calculated from system (2). The system produces different bursting oscillations under certain parameter conditions, with the excitation amplitude adjusted. We have obtained the phase diagram and time history diagram of the following types of bursting oscillations: fold-fold, fold-subHopf, supHopf-supHopf, and homoclinic-homoclinic.

Acknowledgment

The work described in this paper is supported by Yunnan Fundamental Research Project (No. 202501AS070161).

References

[1] Prandtl, L., Motion of Fluids with Very Little Viscosity, Technical Memo-452, NACA, Washington, DC, 1928
[2] Yang, W., Towfighian, S., A Parametric Resonator with Low Threshold Excitation for Vibration Energy Harvesting, *Journal of Sound and Vibration, 446* (2019), Apr., pp. 129-143
[3] Beims, M. W., Gallas, J. A. C., Predictability of the Onset of Spiking and Bursting in Complex Chemical Reactions, *Physical Chemistry Chemical Physics, 20* (2018), 27, pp. 18539-18546
[4] Theodosiou, C., *et al.*, Periodic Steady State Response of Large Scale Mechanical Models with Local Non-linearities,. *International Journal of Solids and Structures, 46* (2009), 20, pp. 3565-3576
[5] Yang, S. C., Hong, H. P., Non-Linear Inelastic Responses of Transmission Tower-Line System Under Downburst Wind, *Engineering Structures, 123* (2016), 15, pp. 490-500
[6] Zhang, L., *et al.*, Chaos Control for the Periodically Excited Van der Pol-Duffing. *Journal of Wenzhou University·Natural Sciences, 28* (2007), 2, pp. 11-14
[7] Ma, X. D., *et al.*, Complex Mixed-Mode Vibration Types Triggered by the Pitchfork Bifurcation Delay in a Driven Van der Pol-Duffing Oscillator, *Applied Mathematics and Computation, 411* (2021), 126522
[8] He, C. H., El-Dib, Y. O., A Heuristic Review on the Homotopy Perturbation Method for Non-conservative Oscillators, *Journal of Low Frequency Noise, Vibration & Active Control, 41* (2022), 2, pp. 572-603
[9] He, C. H., *et al.*, Controlling the Kinematics of a Spring-Pendulum System Using an Energy Harvesting Device, *Journal of Low Frequency Noise, Vibration & Active Control, 41* (2022), 3, pp. 1234-1257
[10] Liu, Y. B., Chen, Y. S., Global Bifurcations for a Generalized Codimension-4 Duffing-Van der Pol Equation, *Journal of Vibration and Shock, 30* (2011), 1, pp. 69-72
[11] He, C. H., *et al.*, Hybrid Rayleigh-Van der Pol-Duffing Oscillator: Stability Analysis and Controller, *Journal of Low Frequency Noise, Vibration & Active Control, 41* (2022), 1, pp. 244-268
[12] He, J.-H., El-Dib, Y. O., The Reducing Rank Method to Solve Third-Order Duffing Equation with the Homotopy Perturbation, *Numerical Methods for Partial Differential Equations, 37* (2021), 2, pp. 1800-1808
[13] He, J.-H., *et al.*, Homotopy Perturbation Method for fractal Duffing Oscillator with Arbitrary Conditions, *Fractals, 30* (2022), 9, 22501651
[14] He, J.-H., *et al.*, A Good Initial Guess for Approximating Non-Linear Oscillators by the Homotopy Perturbation Method, *Facta Universitatis, Series: Mechanical Engineering, 21* (2023), 1, pp. 21-29
[15] Anjum, N., *et al.*, Free Vibration of a Tapered Beam by the Aboodh Transform-Based Variational Iteration Method, *Journal of Computational Applied Mechanics, 55* (2024), 3, pp. 440-450
[16] Tang, W., *et al.*, Variational Iteration Method for the Nanobeams-Based N/MEMS System, *MethodsX, 11* (2023), 102465
[17] He, J.-H., The Simplest Approach to Non-Linear Oscillators, *Results in Physics, 15* (2019), 102546
[18] Zhang, J. G., *et al.*, Application of He's Frequency Formula to Non-Linear Oscillators with Generalized Initial Conditions, *Facta Universitatis, Series: Mechanical Engineering, 21* (2023), 4, pp. 701-712
[19] Kaid, N., *et al.*, Enhancing Thermal Comfort in Building Innovations in Sustainable Cooling and Heating Systems Utilizing Geothermal Energy, *Thermal Science, 27* (2023), 4B, pp. 3477-3486
[20] Yau, H. T., *et al.*, Proximal Policy Optimization-Based Controller for Chaotic Systems, *International Journal of Robust and Non-linear Control, 34* (2024), 1, pp. 586-601
[21] Kuo, P.-H., *et al.*, Novel Fractional-Order Convolutional Neural Network Based Chatter Diagnosis Approach in Turning Process with Chaos Error Mapping, *Non-linear Dynamics, 111* (2023), 8, pp. 7547-7564
[22] Kuo, P.-H., *et al.*, Machine Tool Chattering Monitoring by Chen-Lee Chaotic System-Based Deep Convolutional Generative Adversarial Nets, *Structural Health Monitoring, 22* (2023), 6, pp. 3891-3907
[23] He, J.-H., *et al.*, Pull-Down Instability of the Quadratic Non-Linear Oscillators, *Facta Universitatis, Series: Mechanical Engineering, 21* (2023), 2, pp. 191-200

[24] He, J.-H., *et al.*, Pull-in Stability of a Fractal MEMS System and Its Pull-In Plateau, *Fractals, 30* (2022), 9, 22501857
[25] He, J.-H., *et al.*, Piezoelectric Biosensor Based on Ultrasensitive MEMS System, *Sensors and Actuators: A. Physical., 376* (2024), 115664
[26] Tian, D., *et al.*, Fractal N/MEMS: From Pull-in Instability to Pull-in Stability, *Fractals*, *29* (2021), 2, 2150030
[27] Tian, D., He, C. H., A Fractal Micro-Electromechanical System and Its Pull-in Stability, *Journal of Low Frequency Noise Vibration and Active Control*, *40* (2021), 3, pp. 1380-1386
[28] He, C. H., A Variational Principle for a Fractal Nano/Microelectromechanical (N/MEMS) System, *Int. J. Numer. Method. H*., *33* (2023), 1, pp. 351-359
[29] Zhang, L., Wang, T., Qualitative Properties, Bifurcations and Chaos of a Discrete Predator-Prey System with Weak Allee Effect on the Predator, *Chaos, Solitons & Fractals*, *175* (2023), Oct., 113995
[30] Hastir, A., Muolo, R., A Generalized Routh-Hurwitz Criterion for the Stability Analysis of Polynomials with Complex Coefficients: Application to the PI-control of Vibrating Structures, *IFAC Journal of Systems and Control*, *26* (2023), 100235
[31] Zhang, X. Y., *et al.*, Bursting Oscillations Induced by Coexisted Cycles Separated by Fold Limit Cycle Bifurcation, *Journal of Vibration Engineering & Technologies*, *12* (2024), Suppl. 1, pp. S573-S583
[32] Hou, H. S., *et al.*, On Fractional Ring Neural Networks with Multiple Time Delays: Stability and Hopf Bifurcation Analysis, *Chinese Journal of Physics, 90* (2024), Aug., pp. 303-318
[33] Gjata, O., Zanolin, F., An Application of the Melnikov Method to a Piecewise Oscillator, *Contemp. Math., 4* (2024), 2, pp. 249-269
[34] Colombo, G., *et al.*, Inflated Deterministic Chaos and Smale's Horseshoe, *Journal of Difference Equations and Applications, 18* (2012), 3, pp. 471-488

Paper submitted: December 25, 2023
Paper revised: July 6, 2024
Paper accepted: July 6, 2024